Monthly Notices of the ROYAL ASTRONOMICAL SOCIETY

MNRAS **542,** 902–916 (2025) https://doi.org/10.1093/mnras/staf1295
Advance Access publication 2025 August 7

Spectropolarimetry of synchrotron radiation from relativistic electrons with anisotropic pitch-angle and various energy distributions

Paul C. W. Lai [1]★ Kaye J. Li [1] Y. X. Jane Yap [1,2]★ Kinwah Wu [1,3,4,5]★ and Albert K. H. Kong [2]

[1]*Mullard Space Science Laboratory, University College London, Holmbury St Mary, Surrey RH5 6NT, UK*
[2]*Institute of Astronomy, National Tsing Hua University, Hsinchu 30013, Taiwan (R.O.C.)*
[3]*Research School of Astronomy and Astrophysics, Australian National University Canberra ACT 2611, Australia*
[4]*Department of Physics, Chinese University of Hong Kong, Shatin, NT, Hong Kong SAR, China*
[5]*Kavli Institute for the Physics and Mathematics of the Universe (WPI), UTIAS, The University of Tokyo, Kashiwa, Chiba 277-8583, Japan*

Accepted 2025 August 5. Received 2025 August 1; in original form 2025 June 25

ABSTRACT

For synchrotron radiation from relativistic electrons having a power-law energy distribution with a power-law index p in an optically thin medium with a locally uniform magnetic field, it is generally adopted that the spectral index $\alpha = (p-1)/2$ and the degree of linear polarization $\Pi_{\rm L,pl} = (p+1)/(p+7/3)$, and hence that $\Pi_{\rm L,pl} = (\alpha+1)/(\alpha+5/3)$. These $(\alpha, \Pi_{\rm L,pl}; p)$ relations are derived assuming that the electrons have an isotropic momentum distribution and a power-law energy distribution, and they have been used, almost universally, in the interpretation of polarimetry observations. In this study, we assess the validity of the $(\alpha, \Pi_{\rm L,pl}; p)$ relations in different scenarios, such as anisotropic electron momenta and non-power-law distributions of electron energy. We calculate the synchrotron radiation and polarization spectra for power-law, kappa, and log-parabola electron-energy distributions, with isotropic and two anisotropic (beamed and loss cone) electron-momentum distributions. Our calculations show that when the electron momenta are isotropic, the usual $(\alpha, \Pi_{\rm L,pl}; p)$ relations are generally applicable. However, if the electrons are anisotropic, the usual $(\alpha, \Pi_{\rm L,pl}; p)$ relations could break down. Applying the usual $(\alpha, \Pi_{\rm L,pl}; p)$ relations indiscriminately without caution on anisotropy in the electron momentum distribution, would lead to incorrect interpretatsions of polarimetry data.

Key words: polarization – radiation mechanisms: non-thermal – radiative transfer.

1 INTRODUCTION

Synchrotron radiation, emitted when relativistic charged particles gyrating around a magnetic field, is a common radiative process in astrophysical environments. A characteristic of synchrotron radiation is its strong linear polarization but negligible circular polarization. The spectrum of synchrotron radiation from an ensemble of relativistic electrons with an isotropic extended power-law energy distribution, $\mathrm{d}n_{\rm e}(\gamma)/\mathrm{d}\gamma \propto \gamma^{-p}$ [where $n_e(\gamma)$ is the electron number density,[1] γ is the Lorentz factor of the electrons], of energy index p is also a power law, in the optical thin regime, and the specific intensity, at frequency ν, is given by $I_\nu \propto \nu^{-\alpha}$. where $\alpha = (p-1)/2$ (see e.g. Tucker 1975; Rybicki & Lightman 1979). In the optically thick regime, the emission spectrum also follows a power law but with a different spectral index of $\alpha = -5/2$, which is independent of the electron energy distribution (Ginzburg & Syrovatskii 1965, 1969). The degree of linear polarization or the linear polarization degree (polarization degree or PD hereafter) is

$$\Pi_{\rm L,pl} = \frac{p+1}{p+7/3} = \frac{\alpha+1}{\alpha+5/3} \tag{1}$$

for optically thin emission and $\Pi^{\rm thick}_{\rm L,pl} = 3/(6p+13)$ for optically thick emission (Ginzburg & Syrovatskii 1969). These expressions are derived with the assumption of a uniform magnetic field orderly aligned in the emission region, and the polarization vector is thus perpendicular to the orientation of the magnetic field $\boldsymbol{B}$. They are applicable to other charged leptons and charged baryons besides electrons.

These expressions have been commonly used in astronomy, for the interpretation of the polarized radiation from a variety of non-thermal sources, including jets from active galactic nuclei (AGNs), X-ray binaries, gamma-ray bursts, and diffuse emission from extended systems such as supernova remnants and pulsar-wind nebulae (e.g. Coburn & Boggs 2003; Perlman et al. 2011; Lai, Ng & Bucciantini 2022; Kaaret et al. 2024; Slane et al. 2024).

Power-law-like energy distributions of charged particles can be generated from *Fermi* I process (e.g. in diffusive shocks) and *Fermi* II process (e.g. in randomly moving deflectors/reflectors). A perfect

★ E-mail: chong.lai.22@ucl.ac.uk (PCWL); yapyeexuan@gapp.nthu.edu.tw (YXJY); kinwah.wu@ucl.ac.uk (KW)

[1]The number density of electrons with energy in the range (γ_1, γ_2), at a given location, is

$$n_{\rm e} = \int_{\gamma_1}^{\gamma_2} \mathrm{d}\gamma \left(\frac{\mathrm{d}n_{\rm e}(\gamma)}{\mathrm{d}\gamma}\right) .$$

Note that in some literature, the expression $\mathrm{d}n_{\rm e}(\gamma)/\mathrm{d}\gamma$ that we adopt here is referred to as '$n_{\rm e}(\gamma)$'.

power-law energy distribution for the emitting charged particles is, however, an idealized situation. Radiative cooling and processes such as episodic injections of high-energy particles would modify the particle energy distribution, even if the energy distribution is a perfect power law initially. None the less, for the analysis at fixed wavelength-band observations, using a power-law distribution for computing the emission spectrum and polarization is still a reasonable approximation in most situations (which we will demonstrate in the later sections).

Note that the emitting charged particles were assumed to have an isotropic momentum pitch-angle distribution (hereafter pitch-angle distribution), with respect to the orientation of the magnetic field, in the rest frame of the infinitesimal volume containing the particles when deriving the above expressions. This assumption provides a great simplification in deriving the angle-dependent polarization components of the radiation – the emission, absorption and other radiative transfer coefficients.[2] With the advancement in the broad multiband polarimetric observations and the new polarization data obtained in high-energy domains, e.g. current observations in the keV X-rays by the Imaging X-ray Polarimetry Explorer (IXPE; see Soffitta et al. 2021; Weisskopf et al. 2022), it is timely to revisit how the polarization in the synchrotron radiation changes when relativistic charged particles do not have an isotropic pitch-angle distribution and do not have a power-law energy distribution. Recent studies (Yang & Zhang 2018; Comisso, Sobacchi & Sironi 2020) have demonstrated that we cannot directly infer the electron energy spectral index p from the observed synchrotron spectral index α if the emitting electron momenta do not have an isotropic distribution. We extend the work of Yang & Zhang (2018) by calculating the polarizations of the synchrotron radiation from a variety of anisotropic electron momentum distributions that are relevant to astrophysical applications. We organize the paper as follows. We present in Section 2 the derivations of the emissivities and polarization for synchrotron radiation from relativistic charged particles, relaxing the usual assumptions of an extended power-law energy distributions and of isotropic pitch-angle distributions, and we show in Section 3 the results. We discuss the astrophysical implications in Section 4. A summary is given in Section 5.

2 SYNCHROTRON RADIATION FROM RELATIVISTIC ELECTRONS

2.1 Radiative power and polarization

Synchrotron radiation is anisotropic, with the observed intensity depending on the line of sight to the observer with respect to the orientation of the magnetic field and travelling direction of the charged particles in the emission region. Suppose the radiation propagating in the direction $\hat{\boldsymbol{n}}$ along the line of sight and the magnetic field $\boldsymbol{B}$ is locally uniform and aligned with the z-axis. We can then decompose the power of synchrotron radiation into two orthogonal components, designated as the perpendicular component and the parallel component. The perpendicular component corresponds to the electromagnetic waves whose electric field unit vector $\hat{\boldsymbol{\epsilon}}_\perp$ perpendicular to the magnetic field $\boldsymbol{B}$ and $\hat{\boldsymbol{n}}$, and the parallel component to the electromagnetic waves with the electric field unit vector given by $\hat{\boldsymbol{\epsilon}}_\parallel = \hat{\boldsymbol{n}} \times \hat{\boldsymbol{\epsilon}}_\perp$. The power of the two components of synchrotron radiation from an electron with a Lorentz factor γ are[3]

$$\frac{\mathrm{d}W_\perp}{\mathrm{d}\omega\,\mathrm{d}\Omega}(\omega,\tilde{\theta},\tilde{\alpha},\gamma) = \left(\frac{\omega_B}{2\pi}\right)\frac{e^2}{3\pi^2 c}\left(\frac{\omega\rho}{c}\right)^2\left(\frac{1}{\gamma^2}+\tilde{\theta}^2\right)^2[K_{2/3}(\xi)]^2\,, \quad (2)$$

$$\frac{\mathrm{d}W_\parallel}{\mathrm{d}\omega\,\mathrm{d}\Omega}(\omega,\tilde{\theta},\tilde{\alpha},\gamma) = \left(\frac{\omega_B}{2\pi}\right)\frac{e^2}{3\pi^2 c}\left(\frac{\omega\rho}{c}\right)^2\tilde{\theta}^2\left(\frac{1}{\gamma^2}+\tilde{\theta}^2\right)[K_{1/3}(\xi)]^2 \quad (3)$$

(see e.g. Rybicki & Lightman 1979; Yang & Zhang 2018), where ω is the angular frequency of the radiation, $\tilde{\alpha}$ is the angle between the electron momentum and the magnetic field (the pitch angle), $\tilde{\theta}$ is the angle between $\hat{\boldsymbol{n}}$ and the instantaneous-trajectory plane, $\omega_B = eB/(\gamma m_e c)$ is the gyro frequency, $\rho = c/(\omega_B \sin\tilde{\alpha})$ is the radius of the electron's helical trajectory, K_a is the modified Bessel function of the second kind with order a, $\xi = (1/\gamma^2 + \tilde{\theta}^2)^{3/2}(\omega\rho)/(3c)$, and $B = |\boldsymbol{B}|$. The total power of the radiation is given by

$$\frac{\mathrm{d}W_{\rm tot}}{\mathrm{d}\omega\,\mathrm{d}\Omega}(\omega,\tilde{\theta},\tilde{\alpha},\gamma) = \frac{\mathrm{d}W_\perp}{\mathrm{d}\omega\,\mathrm{d}\Omega} + \frac{\mathrm{d}W_\parallel}{\mathrm{d}\omega\,\mathrm{d}\Omega}\,, \quad (4)$$

and the power of the linearly polarized radiation by

$$\frac{\mathrm{d}W_{\rm pol}}{\mathrm{d}\omega\,\mathrm{d}\Omega}(\omega,\tilde{\theta},\tilde{\alpha},\gamma) = \frac{\mathrm{d}W_\perp}{\mathrm{d}\omega\,\mathrm{d}\Omega} - \frac{\mathrm{d}W_\parallel}{\mathrm{d}\omega\,\mathrm{d}\Omega}\,. \quad (5)$$

As the perpendicular component is larger than the parallel component, the linear polarization of synchrotron radiation is always perpendicular to the magnetic field direction at the location of emission.

The total power of the emission from an ensemble of electrons is the sum of the radiative power of individual electrons (for negligible self-absorption). We denote the electron number distribution function as $N_e(\gamma,\tilde{\alpha})$. The specific flux of synchrotron radiation from an ensemble of electrons, measured by an observer located at distance D, is[4]

$$\begin{aligned} F_\omega(\omega,\theta) &= \frac{2\pi}{D^2}\int_0^\pi \mathrm{d}\tilde{\alpha}\ \sin\tilde{\alpha} \\ &\quad \left[\int_{\gamma_{\rm min}}^{\gamma_{\rm max}} \mathrm{d}\gamma\ \frac{\mathrm{d}W_{\rm tot}}{\mathrm{d}\omega\,\mathrm{d}\Omega}(\omega,\tilde{\alpha}-\theta,\tilde{\alpha},\gamma)N_e(\gamma,\tilde{\alpha})\right] \\ &= \frac{2\pi}{D^2}\int_{-\theta}^{\pi-\theta} \mathrm{d}\tilde{\theta}\ \sin(\tilde{\theta}+\theta) \\ &\quad \left[\int_{\gamma_{\rm min}}^{\gamma_{\rm max}} \mathrm{d}\gamma\ \frac{\mathrm{d}W_{\rm tot}}{\mathrm{d}\omega\,\mathrm{d}\Omega}(\omega,\tilde{\theta},\tilde{\theta}+\theta,\gamma)N_e(\gamma,\tilde{\theta}+\theta)\right]\,, \quad (6) \end{aligned}$$

[2]With the emission, absorption and Faraday transfer coefficients defined in the local rest frame of the infinitesimal emission volume, one can execute the radiative transfer calculations using ray-tracing algorithms, in a covariant manner (see Fuerst & Wu 2004; Younsi, Wu & Fuerst 2012) for systems with large differential special relativistic motion (see appendix A in Saxton et al. 2010), under extreme gravity (see e.g. Prather et al. 2023) or in cosmological expansion (see Chan et al. 2019; On et al. 2019).

[3]As discussed in Rybicki & Lightman (1979), there would be an additional factor of $1/\sin^2\tilde{\alpha}$ for the received power if electrons move in perfect helical motion around a magnetic field line. In astrophysical environments, magnetic fields are hardly perfectly uniform and ordered. Electrons would move in curved helical orbits along the magnetic field line, and they can bounced back and forth by magnetic mirroring effect. As such we should expect the received power and the emitted power to match each other. An additional factor of $1/\sin^2\tilde{\alpha}$ is therefore unnecessary in the astrophysical applications.

[4]The subscript ω here represents per unit angular frequency ω, i.e. the specific flux $F_\omega = \mathrm{d}F/\mathrm{d}\omega$, where F is the flux of the radiation integrated over the relevant range of ω (cf. $\mathrm{d}W/\mathrm{d}\omega$ in equations 4 and 5).

and the corresponding polarized specific flux is

$$F_{\omega,\mathrm{pol}}(\omega,\theta) = \frac{2\pi}{D^2}\int_0^{\pi} \mathrm{d}\tilde{\alpha}\ \sin\tilde{\alpha} \left[\int_{\gamma_{\min}}^{\gamma_{\max}} \mathrm{d}\gamma\ \frac{\mathrm{d}W_{\mathrm{pol}}}{\mathrm{d}\omega\,\mathrm{d}\Omega}(\omega,\tilde{\alpha}-\theta,\tilde{\alpha},\gamma)N_e(\gamma,\tilde{\alpha})\right] = \frac{2\pi}{D^2}\int_{-\theta}^{\pi-\theta} \mathrm{d}\tilde{\theta}\ \sin(\tilde{\theta}+\theta) \left[\int_{\gamma_{\min}}^{\gamma_{\max}} \mathrm{d}\gamma\ \frac{\mathrm{d}W_{\mathrm{pol}}}{\mathrm{d}\omega\,\mathrm{d}\Omega}(\omega,\tilde{\theta},\tilde{\theta}+\theta,\gamma)N_e(\gamma,\tilde{\theta}+\theta)\right], \tag{7}$$

where θ is the angle between the line-of-sight directional unit vector $\hat{\boldsymbol{n}}$ to the observer and the magnetic field $\boldsymbol{B}$.

If the electrons have an isotropic pitch-angle distribution with respect to the magnetic field, i.e. $N_e(\gamma,\tilde{\alpha})$ does not depend on $\tilde{\alpha}$, the two integrals are separable. We first execute the integral over $\tilde{\theta}$, which is

$$\frac{\mathrm{d}W_{\mathrm{mono}}}{\mathrm{d}\omega}(\omega,\theta,\gamma) = 2\pi\int_{-\theta}^{\pi-\theta} \mathrm{d}\tilde{\theta}\ \sin(\tilde{\theta}+\theta)\ \frac{\mathrm{d}W_{\mathrm{tot}}}{\mathrm{d}\omega\,\mathrm{d}\Omega}(\omega,\tilde{\theta},\tilde{\theta}+\theta,\gamma)\,. \tag{8}$$

As the emission is highly concentrated around $\tilde{\theta}=0$, we may consider an approximation to this integral following Westfold (1959) and Rybicki & Lightman (1979)

$$\frac{\mathrm{d}W_{\mathrm{mono}}}{\mathrm{d}\omega}(\omega,\theta,\gamma) \approx 2\pi\int_{-\infty}^{+\infty} \mathrm{d}\tilde{\theta}\ \sin\theta\ \frac{\mathrm{d}W_{\mathrm{tot}}}{\mathrm{d}\omega\,\mathrm{d}\Omega}(\omega,\tilde{\theta},\theta,\gamma) = \frac{\sqrt{3}e^3 B\sin\theta}{2\pi m_e c^2}F(x)\,, \tag{9}$$

with $x=(\omega/\omega_c)$, $\omega_c=(3/2)\gamma^3\omega_B\sin\tilde{\alpha}$, and $F(x)=x\int_x^{\infty}\mathrm{d}\xi\ K_{5/3}(\xi)$. Similarly, we obtain for the linear polarization that

$$\frac{\mathrm{d}W_{\mathrm{mono,pol}}}{\mathrm{d}\omega}(\omega,\theta,\gamma) \approx 2\pi\int_{-\infty}^{+\infty} \mathrm{d}\tilde{\theta}\ \sin\theta\ \frac{\mathrm{d}W_{\mathrm{pol}}}{\mathrm{d}\omega\,\mathrm{d}\Omega}(\omega,\tilde{\theta},\theta,\gamma) = \frac{\sqrt{3}e^3 B\sin\theta}{2\pi m_e c^2}G(x)\,, \tag{10}$$

where $G(x)=xK_{2/3}(x)$.

With the approximation above, the specific flux of synchrotron radiation from electrons with isotropic distribution can be simplified to

$$F_{\omega}(\omega,\theta) = \frac{1}{4\pi D^2}\frac{\sqrt{3}e^3 B\sin\theta}{2\pi m_e c^2}\int_{\gamma_{\min}}^{\gamma_{\max}}\mathrm{d}\gamma\ F(\omega/\omega_c)\frac{\mathrm{d}N_e(\gamma)}{\mathrm{d}\gamma}\,; \tag{11}$$

$$F_{\omega,\mathrm{pol}}(\omega,\theta) = \frac{1}{4\pi D^2}\frac{\sqrt{3}e^3 B\sin\theta}{2\pi m_e c^2}\int_{\gamma_{\min}}^{\gamma_{\max}}\mathrm{d}\gamma\ G(\omega/\omega_c)\frac{\mathrm{d}N_e(\gamma)}{\mathrm{d}\gamma}\,, \tag{12}$$

where $N_e(\gamma,\tilde{\alpha})=(4\pi)^{-1}(\mathrm{d}N_e/\mathrm{d}\gamma)$ for isotropic distributions. For anisotropic distributions, it is necessary to use equations (6) and (7). In astronomy, the synchrotron fluxes are more commonly expressed in term of frequency ν instead of the angular frequency ω, and $F_\nu(\nu)=2\pi F_\omega(\omega)$ with $\nu=\omega/(2\pi)$.

2.2 Electron energy distribution functions

We consider an electron distribution function that depends on the particle energy and the momentum pitch angle with respect to the magnetic field. We consider a function $N_e(\gamma,\tilde{\alpha})$ that can be decomposed into two functions $f_e(\gamma)$ and $g_e(\tilde{\alpha})$, i.e.

$$\frac{\mathrm{d}N_e(\gamma,\tilde{\alpha})}{\mathrm{d}\gamma\,\mathrm{d}\Omega} = N_{e,0}\ f_e(\gamma)\,g_e(\tilde{\alpha})\,, \tag{13}$$

where $N_{e,0}$ is the total number of electrons in the entire emitting volume, and the normalizations are

$$\int_1^{\infty}\mathrm{d}\gamma\ f_e(\gamma) = 2\pi\int_0^{\pi}\mathrm{d}\tilde{\alpha}\ \sin\tilde{\alpha}\ g_e(\tilde{\alpha}) = 1\,. \tag{14}$$

In this study, we consider the generic cases of power-law, broken power-law, and double power-law distributions, and two additional cases of kappa and log-parabola distributions for their relevance for astrophysical applications. The kappa distribution was introduced to provide fits to data from the solar wind observations. It was later adopted by astrophysicists, as it smoothly connects the thermal and non-thermal particle components (see e.g. Davelaar et al. 2018; Event Horizon Telescope Collaboration 2022; Fromm et al. 2022). The log-parabola distribution is used to provide fits to the blazar emission spectrum in some studies (Landau et al. 1986; Krennrich et al. 1999; Massaro et al. 2004; Dermer et al. 2014). This distribution can be generated by certain particle acceleration mechanisms (see Kardashev 1962; Massaro et al. 2004; Tramacere, Massaro & Cavaliere 2007). In addition, we calculate the synchrotron spectrum assuming all electrons have the same energy. This case is unrealistic for astrophysical applications, but an interesting theoretical case study. The result is presented in Appendix A.

2.2.1 *Power law*

An extended power law is one of the generic particle distributions used in astrophysical calculation. We adopt

$$f_e(\gamma) = \frac{(p-1)}{{\gamma_1}^{1-p}-{\gamma_2}^{1-p}}\gamma^{-p} \tag{15}$$

for the power-law energy distribution in our calculations, with the particle energies $\gamma_1\le\gamma\le\gamma_2$ and the power-law index $p>1$.

2.2.2 *Broken power law and double power law*

Often in many astrophysical situations, the particle energy spectrum could not be represented by an extended power law. A common extension of the extended power-law model is a spectrum jointed by two power laws with different energy spectral indices. Such spectrum can be represented mathematically as

$$f_e(\gamma) = \frac{1}{\gamma_b}\left(\frac{{\gamma_b}^{p_1-1}-1}{p_1-1}+\frac{1}{p_2-1}\right)^{-1} \times\left[\mathrm{H}(\gamma_b-\gamma)\left(\frac{\gamma}{\gamma_b}\right)^{-p_1}+\mathrm{H}(\gamma-\gamma_b)\left(\frac{\gamma}{\gamma_b}\right)^{-p_2}\right], \tag{16}$$

(for $\gamma\ge 1$ and $p_1, p_2 > 1$), where $\mathrm{H}(x)$ is the Heaviside step function, whose value is 0 when $x<0$ and 1 when $x\ge 0$. For energy spectral index p taking a larger value at higher energies ($p_2>p_1$), the spectrum is generally referred to as a broken power law. A broken power law could be intrinsic to the acceleration process (see e.g. Comisso 2024), or develop gradually from an initially single power law due to more efficient cooling of the higher energy particles, e.g. synchrotron cooling. A particle index p taking a smaller value at higher energies ($p_2<p_1$), on the other hand, may indicate the presence of two populations of particles both with a power-law energy distribution but with a different energy spectral index.

2.2.3 *Kappa distribution*

We may express f_e in the kappa distribution as

$$f_e(\gamma) = \Lambda\gamma\sqrt{\gamma^2-1}\left(1+\frac{\gamma-1}{\kappa w}\right)^{-(\kappa+1)} \tag{17}$$

(see e.g. Pandya et al. 2016), where Λ is a constant such that $\int_1^\infty \mathrm{d}\gamma\ f_e(\gamma) = 1$. For a sufficiently large γ, it resembles a power-law distribution with $p = \kappa - 1$. For small γ, it resembles a thermal-like distribution with its width regulated by the parameter w.

2.2.4 *Log-parabola distribution*

We may express the log-parabola distribution as

$$f_e(\gamma) = \sqrt{\frac{2}{\pi\sigma_e^2}}\left[\frac{1}{\mathrm{erf}(y_2)-\mathrm{erf}(y_1)}\right]\frac{1}{\gamma}\ \exp\left(\frac{-(\ln(\gamma)-\ln(\gamma_c))^2}{2{\sigma_e}^2}\right), \tag{18}$$

where $\gamma_1 \le \gamma \le \gamma_2$. The parameter $y_i = (\ln(\gamma_i) - \ln(\gamma_c))/\sqrt{2\sigma_e^2}$, with $i = 1$ or 2.

2.3 Electron momentum pitch-angle distribution functions

For the pitch-angle distributions, we consider the idealized case of isotropic distribution and two parametric cases of anisotropic distributions, the beamed particles and the loss cone. Isotropic distribution is often the default assumption in calculations, when we have no knowledge about the pitch-angle distribution. It is justified also in the situation that particle collisions are sufficiently efficient to suppress the development of pitch-angle anisotropy. When the particles are preferentially accelerated towards a particular direction, it results in a particle beam. This can occur, for example, in magnetic reconnection, particles get stronger acceleration along the magnetic field direction, causing a beam-like distribution (see Comisso & Sironi 2019; Comisso & Jiang 2023). A loss-cone distribution could be developed in magnetic mirrors or in converging magnetic-field configurations (Baldwin 1977) where particles with large momentum pitch angles will be trapped but particles with momenta roughly aligned with the magnetic field orientation could escape from the confinement.

2.3.1 *Isotropic momentum pitch-angle distribution*

For isotropic pitch-angle distribution, the function $g_e(\tilde{\alpha})$ is a constant:

$$g_e(\tilde{\alpha}) = \frac{1}{4\pi}\ . \tag{19}$$

2.3.2 *Beamed particles*

For the beamed distribution, it takes the following form

$$g_e(\tilde{\alpha}) = \frac{1}{\sqrt{2\pi^3{\sigma_\alpha}^2}}\left[\frac{1}{\mathrm{erf}(t_2)-\mathrm{erf}(t_1)}\right]\exp\left(-\frac{(\cos\tilde{\alpha}-\cos\tilde{\alpha}_0)^2}{2{\sigma_\alpha}^2}\right), \tag{20}$$

where $t_2 = (1-\cos\tilde{\alpha}_0)/\sqrt{2{\sigma_\alpha}^2}$ and $t_1 = (-1-\cos\tilde{\alpha}_0)/\sqrt{2{\sigma_\alpha}^2}$. The beamwidth is mainly determined by σ_α but also depends on the beaming angle $\tilde{\alpha}_0$. We list the half-width at half-maximum (HWHM) of the beam $\alpha_{\rm HWHM}$ for the parameter values used in our calculations (see Table 1). For $\tilde{\alpha}_0 = 0$, we have $\alpha_{\rm HWHM} = 0.15, 0.27, 0.49$ for $\sigma_\alpha = 10^{-2}, 10^{-1.5}, 10^{-1}$, respectively. For $\tilde{\alpha}_0 = \pi/2$, we have $\alpha_{\rm HWHM} = 0.012, 0.037, 0.12$ for $\sigma_\alpha = 10^{-2}, 10^{-1.5}, 10^{-1}$, respectively. We note that the mathematical expression of this beamed distribution is not a direct result from kinetic modelling but we adopt it for illustration purpose. It is similar to that used in Yang & Zhang (2018), thus allowing us to make comparison with their work. We also calculated the synchrotron spectrum using the same beamed model in Yang & Zhang (2018), and the result is presented in Appendix B.

Table 1. The HWHM of the beam, $\alpha_{\rm HWHM}$, for different values of $\tilde{\alpha}_0$ and σ_α adopted in the calculations.

	$\sigma_\alpha = 10^{-2}$	$\sigma_\alpha = 10^{-1.5}$	$\sigma_\alpha = 10^{-1}$
$\tilde{\alpha}_0 = 0$	$\alpha_{\rm HWHM} = 0.15$	0.27	0.49
$\tilde{\alpha}_0 = \pi/2$	0.012	0.037	0.12

2.3.3 *Loss cone*

The loss-cone distribution may be considered as a complement of a beamed distribution. We modify the beamed distribution above and model the loss-cone distribution as

$$g_e(\tilde{\alpha}) = \left(4\pi - \sqrt{2\pi^3{\sigma_\alpha}^2}\left[\mathrm{erf}(t_2)-\mathrm{erf}(t_1)\right]\right)^{-1} \times\left(1-\exp\left(-\frac{(\cos\tilde{\alpha}-\cos\tilde{\alpha}_0)^2}{2{\sigma_\alpha}^2}\right)\right). \tag{21}$$

The size of the loss cone is the same as that in the beam model, which is shown in Table 1. We show in Fig. 1 the polar plots of examples of beamed and loss-cone pitch-angle distributions.

3 RESULTS

Without losing generality, we adopt the followings as fiducial values of the total number of electrons, the magnetic field strength, and the distance between the emitting object and the observer in our calculations: $N_{e,0} = 10^{58}$, $B = 1$ mG, and $D = 1$ Gpc. While these are specific values in the calculations, extensive variables such as flux (and flux density) can be obtained by direct scaling. On the other hand, PD is an intensive quantity, which is independent of $N_{e,0}$, D, and also the observing frequency ν when normalized with respect to ν_c.

3.1 Isotropic pitch-angle distributions

Fig. 2 shows the particle distributions, the emission spectra, in terms of the specific flux F_ν, and the degree of linear polarization, PD($\equiv \Pi_{\rm L}$)) (in panels from top to bottom) of synchrotron radiation from relativistic electrons with an isotropic pitch-angle distribution. We found that the degree of linear polarization is well described by a generalized version of equation (1)

$$\Pi_{\rm L,gen} = \frac{\alpha_\nu+1}{\alpha_\nu+5/3}, \tag{22}$$

where $\alpha_\nu = -(\mathrm{d}\log F_\nu/\mathrm{d}\log\nu)$ is the local spectral index, for broken power-law and double power-law energy distributions as in the canonical case of the extended power-law distribution. We refer to equation (22) as the generalized PD formula or the generalized formula hereafter. There is only a small discrepancy, of less than 2 per cent, at the transition between the two power laws in the broken power-law and double power-law energy distributions. Fig. 3 shows the correspondences for three energy distributions: a power law with a high-energy and a low-energy cut-off, kappa

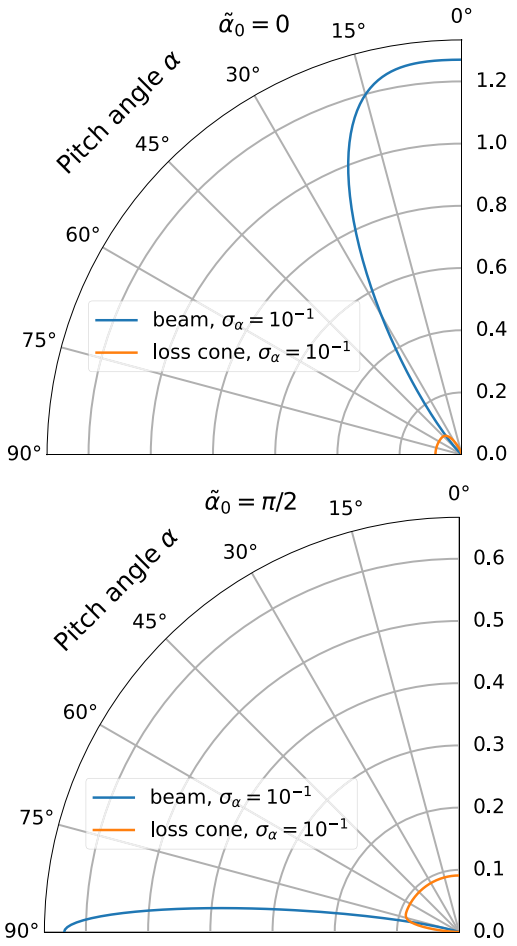

Figure 1. The pitch-angle distribution models used in this paper. $\tilde{\alpha}_0$ specifies the direction of the particle beam or the loss cone; σ_α determines the width of the beam or the loss cone. The upper panel shows a beam and a loss cone pointing along the polar axis ($\tilde{\alpha}_0 = 0$). The lower panel shows a beam and a loss cone, with its axis pointing towards the equatorial plane ($\tilde{\alpha}_0 = \pi/2$).

distribution and log-parabola distributions. As in the cases of extended power-law, broken power-law, and double power-law energy distribution, the same expressions for Π_L are generally applicable when the local value for α_ν is specified. The discrepancies in all cases are at most ∼5 per cent.

3.2 Anisotropic distributions

Here, our focus is on how the anisotropic pitch-angle distribution would alter the spectropolarimetry properties of synchrotron radiation. For illustration we consider only the power-law and kappa distributions for the electron energies. In each case, we calculate $F_\nu(\nu)$ and Π_L for the beamed anisotropy and the loss-cone anisotropy in the electron momentum pitch angle. The results are shown in Fig. 4–7. In all the anisotropic cases considered, the degree of linear polarization is still well described by $\Pi_{L,gen} = (\alpha_\nu + 1)/(\alpha_\nu + 5/3)$ at the high frequency end, but deviates at lower frequencies. The transition frequency that separates these two regimes is different for each case. This could be explained by the nature of beamed radiation of synchrotron radiation. In general, the synchrotron radiation observed is pre-dominantly contributed by a narrow cone of electrons that are traveling close to the direction of the observer, i.e. $\tilde{\alpha} \approx \theta$. We call it the emitting cone hereafter. The angular size of the emitting cone θ_c depends on the electron energy and the observing frequency, given by (Yang & Zhang 2018)

$$\theta_c(\gamma, \nu) \sim \frac{1}{\gamma}\left(\frac{2\nu_c}{\nu}\right)^{1/3} . \tag{23}$$

From equation (23), it can be seen that the emitting cone is smaller for higher frequencies. As long as the pitch-angle distribution function is fairly constant within the emitting cone, whether the pitch-angle distribution function is isotropic outside the cone does not significantly affect the total and polarized flux at that frequency. When going to lower frequencies, the emitting cone becomes larger, and the anisotropy, if exist, will impact the emission spectrum, causing the spectrum to differ from an isotropic case, even when the energy distributions are the same. As the formula $\Pi_{L,gen}$ works well for isotropic cases (see Section 3.1), it should work well for anisotropic cases in the high frequency but not in the low frequency range for the above reason. Unfortunately, the transition frequency cannot be easily worked out or estimated as it depends complexly on the energy distribution function, the pitch-angle distribution function, and the viewing angle. Below we discuss the results of the anisotropic cases in details, and show how the results agree with the above explanation.

3.2.1 *Beamed distribution*

Fig. 4 shows the specific flux $F_\nu(\nu)$ and degree of linear polarization Π_L of synchrotron radiation for electrons that follow a power-law energy distribution with a beamed pitch-angle distribution. In the case that the electrons beam towards the magnetic field direction ($\tilde{\alpha}_0 = 0$), even when the observer is looking right into the beam ($\theta = 0$), the observed flux is weak, especially in the high frequency range. This is because the synchrotron power of an electron scales with $\sin\tilde{\alpha}$. There is no radiation when the electron motion aligns the magnetic field perfectly, and thus the observed flux is weak when $\theta = 0$. The low-frequency emission is less affected by this factor because it is contributed by a wider cone of electrons that has a significant non-zero pitch angle. When the observer gradually looks away from the electron beam, two countering factors start to compete with each other. On one hand, the synchrotron power is stronger for larger $\tilde{\alpha}$, and therefore the observed flux is expected to increase. On the other hand, there are fewer and fewer electrons that point towards the observer when looking away from the beam. The result of these two competing factors is that the observed flux first increases with the viewing angle θ, then gradually decreases after peaking at some sweet spot. For example, for $\tilde{\alpha}_0 = 0$ and $\sigma_\alpha = 10^{-2}$, the observed flux increases from $\theta = 0$ to $\theta = 10\sigma_\alpha$, and gradually drops for $\theta \gtrsim 10\sigma_\alpha$. Lastly, as pointed out in the previous section, the generalized PD formula agrees well with the actual values at high frequency, but deviates at lower frequency. For electron beam with $\tilde{\alpha}_0 = 0$, the transition frequency appears to be insensitive to the electron beamwidth and the viewing angle.

When $\tilde{\alpha}_0 = \pi/2$, the observed flux is the strongest when the observer looks directly into the beam ($\theta = \tilde{\alpha}_0$), and gradually decreases when the observer looks away from the electron beam. The transition frequency is insensitive to the viewing angle, but is lower for a larger electron beam. This is because a beam with larger width is closer to an isotropic distribution for a wider range of pitch angles, making the PD formula $\Pi_{L,gen}$ valid for a larger frequency range.

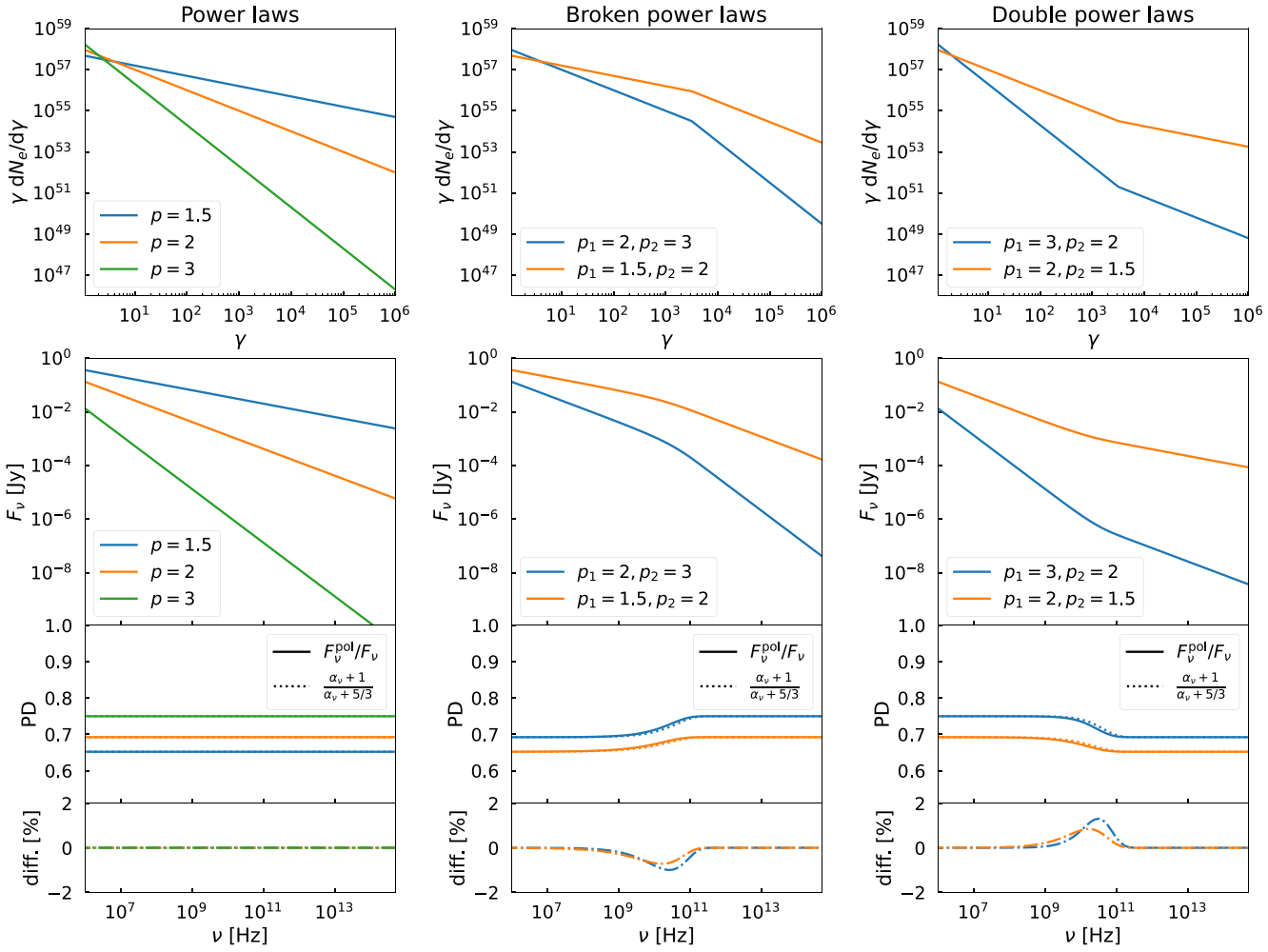

Figure 2. The three columns show the synchrotron spectra and polarization properties of three particle energy distributions, which from left to right are single power law, broken power law, and double power law, assuming an isotropic pitch-angle distribution. The first row shows the particle energy distributions. All the distributions extends from $\gamma = 1$ to infinity. The second row shows the corresponding synchrotron spectrum. The third row shows the frequency-dependent PD. PD is calculated using two different methods. The solid line is calculated using the full formula (equations 11 and 12), and the dotted line is calculated from the local spectral index α_ν (equation 22). The fourth row shows the percentage difference of the PD results between these two methods. The following parameters are used: $\gamma_b = 10^{3.5}$, $\theta = \pi/2$, $N_{e,0} = 10^{58}$, $B = 1$ mG, and $D = 1$ Gpc.

Fig. 5 is the same as Fig. 4 except that the electron energy distribution follows a kappa distribution instead. The results are similar overall and almost identical in the high frequency range. This is due to the property that a kappa energy distribution recovers a power law when the energy is high. The flux density and PD at low frequencies are slightly different but all discussion on the power-law distribution applies to the kappa distribution as well.

3.2.2 *Loss-cone distribution*

Fig. 6 shows the specific flux $F_\nu(\nu)$ and degree of linear polarization $\Pi_{\rm L}$ of synchrotron radiation for electrons that follow a power-law energy distribution with a loss-cone pitch-angle distribution. For any values of $\tilde{\alpha}_0$ and σ_α, the observed flux is the lowest when looking directly into the loss cone ($\theta = \tilde{\alpha}_0$). Also, when $\theta = \tilde{\alpha}_0$, the observed flux is lower for a larger loss cone. These two outcomes showcase that the emission is mainly contributed by particles traveling close to the direction of the observer. Unlike the beamed distribution, the observed flux always increases with the viewing angle for the loss-cone distribution when $\tilde{\alpha}_0 = 0$. This is caused by the increase in particle number for larger pitch angle $\tilde{\alpha}$ and the scaling of synchrotron power with $\sin\tilde{\alpha}$. When $\tilde{\alpha}_0 = 0$, the PD formula $\Pi_{\rm L,gen}$ agrees well with the actual number in the high-frequency range. The transition frequency is lower for larger θ, and $\Pi_{\rm L,gen}$ almost matches the entire frequency range when $\theta = \pi/2$. This is due to the fact that a loss-cone distribution is almost isotropic outside the small loss cone. When $\tilde{\alpha}_0 = 0$ and $\theta = \pi/2$, the spectral energy distribution of the loss-cone distribution is only slightly different from an isotropic distribution.

When $\tilde{\alpha}_0 = \pi/2$, $\Pi_{\rm L,gen}$ gives bad estimation of the PD for some of the cases. For example, when the observer looks directly into the loss cone ($\theta = \tilde{\alpha}_0$), $\Pi_{\rm L,gen}$ is invalid for the entire frequency range. Anisotropy is the main cause of this discrepancy but the interpretation is different depending on the observing frequency considered. In the low frequency range, the emitting cone is so large that the anisotropy is naturally manifested in the spectrum, similar to the reason discussed in the beamed distribution case. In the high frequency range, although the emitting cone is small

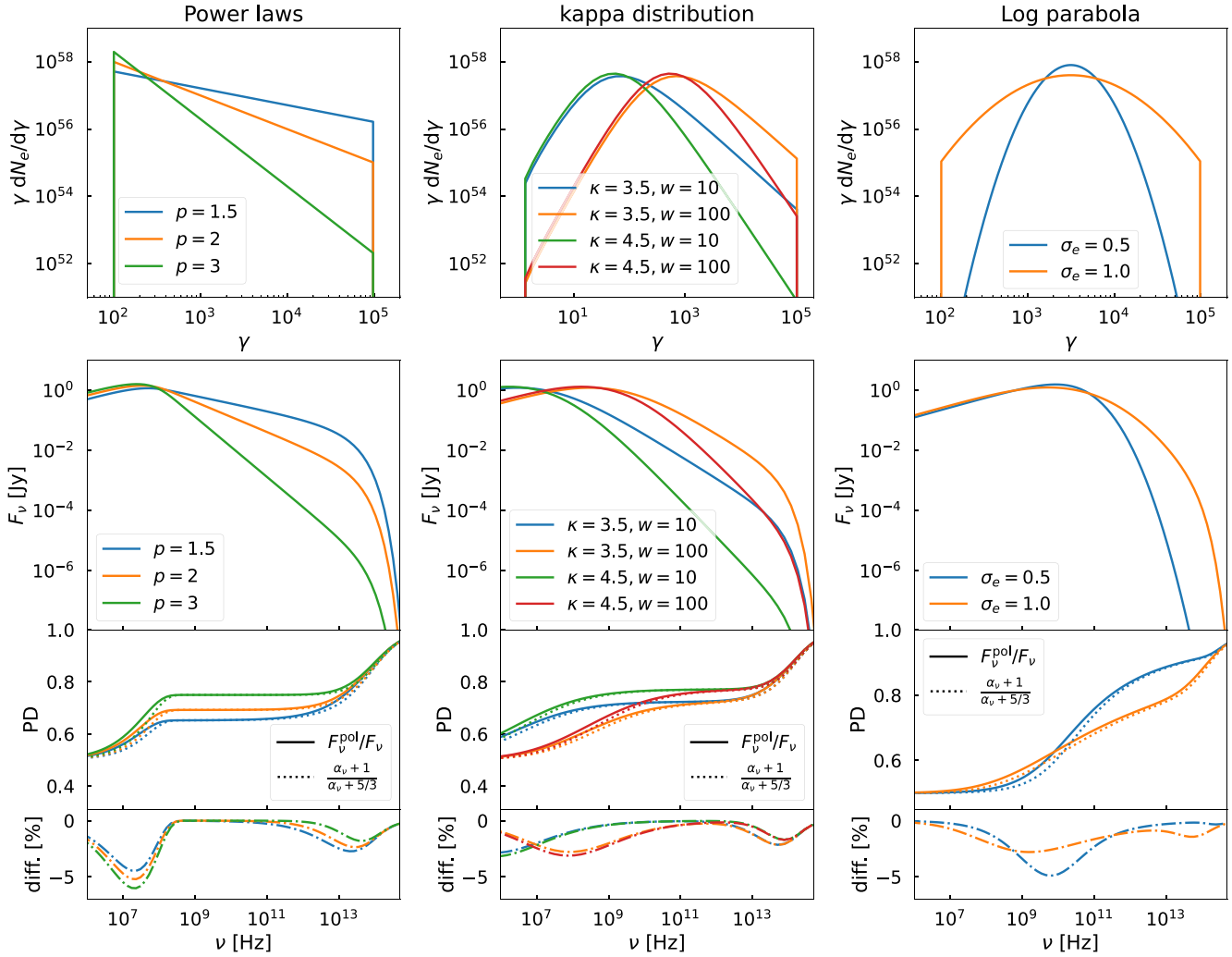

Figure 3. The three columns show the synchrotron spectra and polarization properties of three particle energy distributions, which from left to right are single power law, kappa, and log-parabola, assuming an isotropic pitch-angle distribution. The first row shows the particle energy distributions. All the distributions have a lower cut-off $\gamma_1 = 10^2$ and higher energy cut-off $\gamma_2 = 10^5$. The second row shows the corresponding synchrotron spectrum. The third row shows the frequency-dependent PD. PD is calculated using two different methods. The solid line is calculated using the full formula (equations 11 and 12), and the dotted line is calculated from the local spectral index α_ν (equation 22). The fourth row shows the percentage difference of the PD results between these two methods. The following parameters are used: $\gamma_c = 10^{3.5}$, $\theta = \pi/2$, $N_{e,0} = 10^{58}$, $B = 1$ mG, and $D = 1$ Gpc.

and the pitch-angle distribution is fairly constant within it, there lacks particles inside the emitting cone and the emission mainly comes from particles outside of it. If the spectrum significantly differs from an isotropic distribution, $\Pi_{\rm L,gen}$ will fail to match the real PD. When the observer gradually looks away from the loss cone, $\Pi_{\rm L,gen}$ starts to agree with the actual PD again in the high frequency range, and is almost identical when the viewing direction is far away from the loss cone, e.g. when $\tilde{\alpha}_0 = \pi/2$, $\sigma_\alpha = 10^{-2}$, and $\theta = \tilde{\alpha}_0 - 10\sigma_\alpha$. This is again due to the fact that a loss-cone distribution is almost isotropic outside the small loss cone.

In Fig. 7, the results are calculated using a kappa energy distribution. Overall, the results are similar to the power-law case (Fig. 6), with the high-frequency result being nearly indistinguishable between the two. This similarity arises because the kappa distribution approaches a power-law form at high energies. At lower frequencies, there are minor differences in the flux density and PD, but all conclusions drawn for the power-law distribution remain applicable to the kappa distribution as well.

4 DISCUSSION

4.1 Inhomogeneities in the emission region and propagation effects

The PD calculations presented above, which have put focus on the properties of emission particles, have adopted the following assumptions: (i) the magnetic field in the emission region is uniform structurally and has a well defined value, and (ii) the overall particle density in the emission region is uniform. These assumptions allow us to compute the spectrum and the PD of synchrotron radiation from an ensemble of charged particles unambiguously. We refer the PD obtained in this idealized setting, as intrinsic PD.

We now discuss the effects on the PD of synchrotron radiation and what we would expect for the measured PD when the two assumptions are relaxed. We first examine assumption (i), keeping a uniform particle properties and density across the emission region. This assumption is generally valid, for computing the local emission from within an astrophysical system, when its

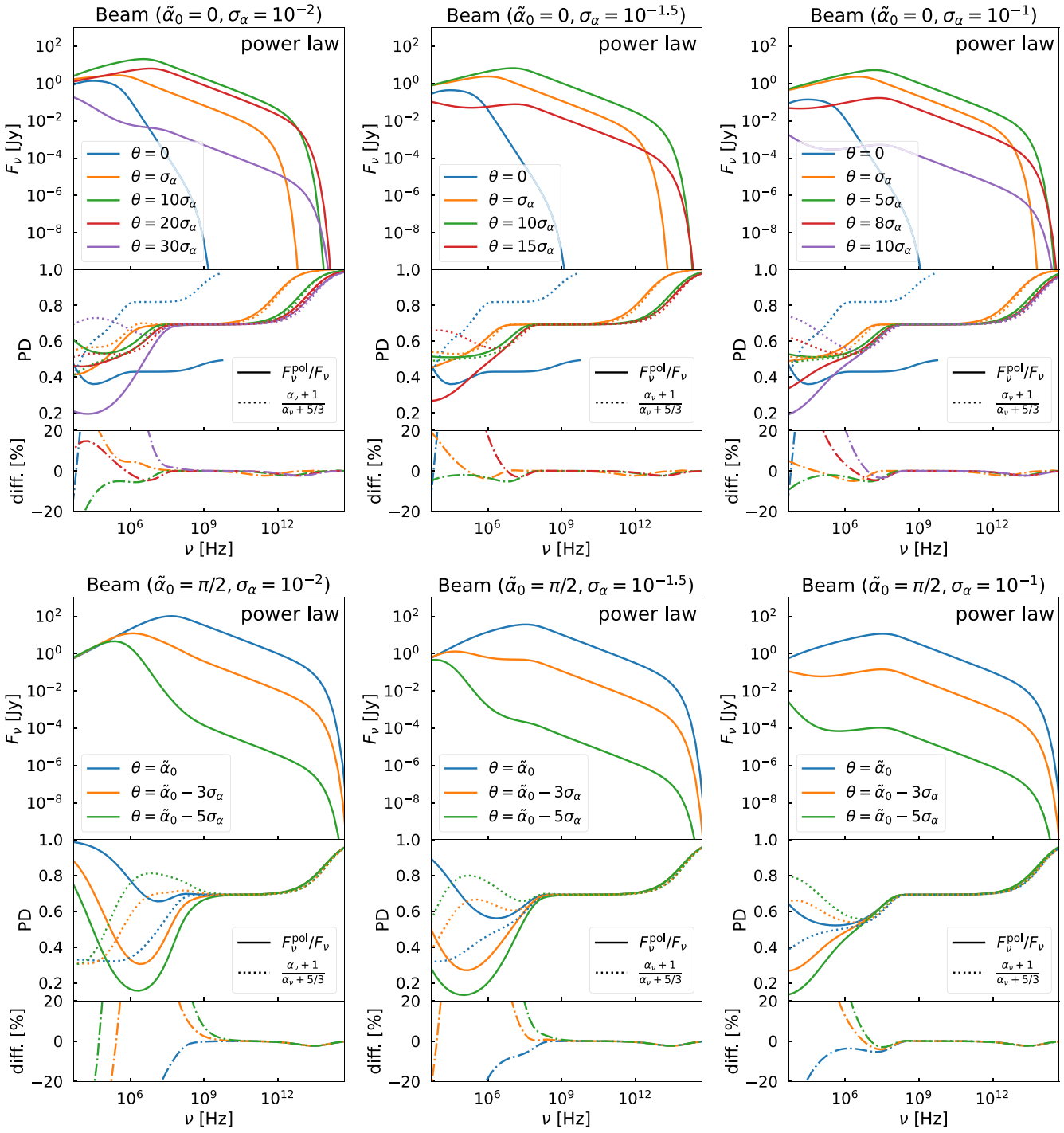

Figure 4. Synchrotron spectra of the beamed model with different values of the parameters, i.e. the beaming direction $\tilde{\alpha}_0$, the opening angle of the beam σ_α, and the viewing angle θ. For all the calculations, electrons are assumed to follow a power-law energy distribution with index $p = 2$, a low-energy cut-off $\gamma_1 = 10^2$, and high-energy cut-off $\gamma_2 = 10^5$. PD is calculated using two methods. The solid line is calculated using the full formula (equations 6 and 7), and the dotted line is calculated from the local spectral index α_ν (equation 22). The beamwidth of these models are $\alpha_{\rm HWHM} = 0.15, 0.27, 0.49, 0.012, 0.037, 0.12$ from left to right, from top to bottom. Besides, the following parameters are used: $N_{e,0} = 10^{58}$, $B = 1$ mG, and $D = 1$ Gpc.

linear size $L > l_{\rm mag} > r_{\rm gyr}$, where $r_{\rm gyr}$ is the gyration radius of the emitting charged particles and $l_{\rm mag}$ is the length-scale over which the magnetic field in the emission region varies. The measured PD will be lower than the intrinsic PD, for a given characteristic strength of the magnetic field in the emission region, as emission from different locations have different orientations of polarization which could partially cancel out each other. Relaxing assumption (ii) has no effect on the PD of the total synchrotron radiation, if the magnetic field is uniform across the emission region and the condition $L \gg r_{\rm gyr}$ holds and the total number of charged emitting particles is fixed, as PD is an intensive quantity. The PD could, however, be significantly affected, as shown in Section 3.2, if

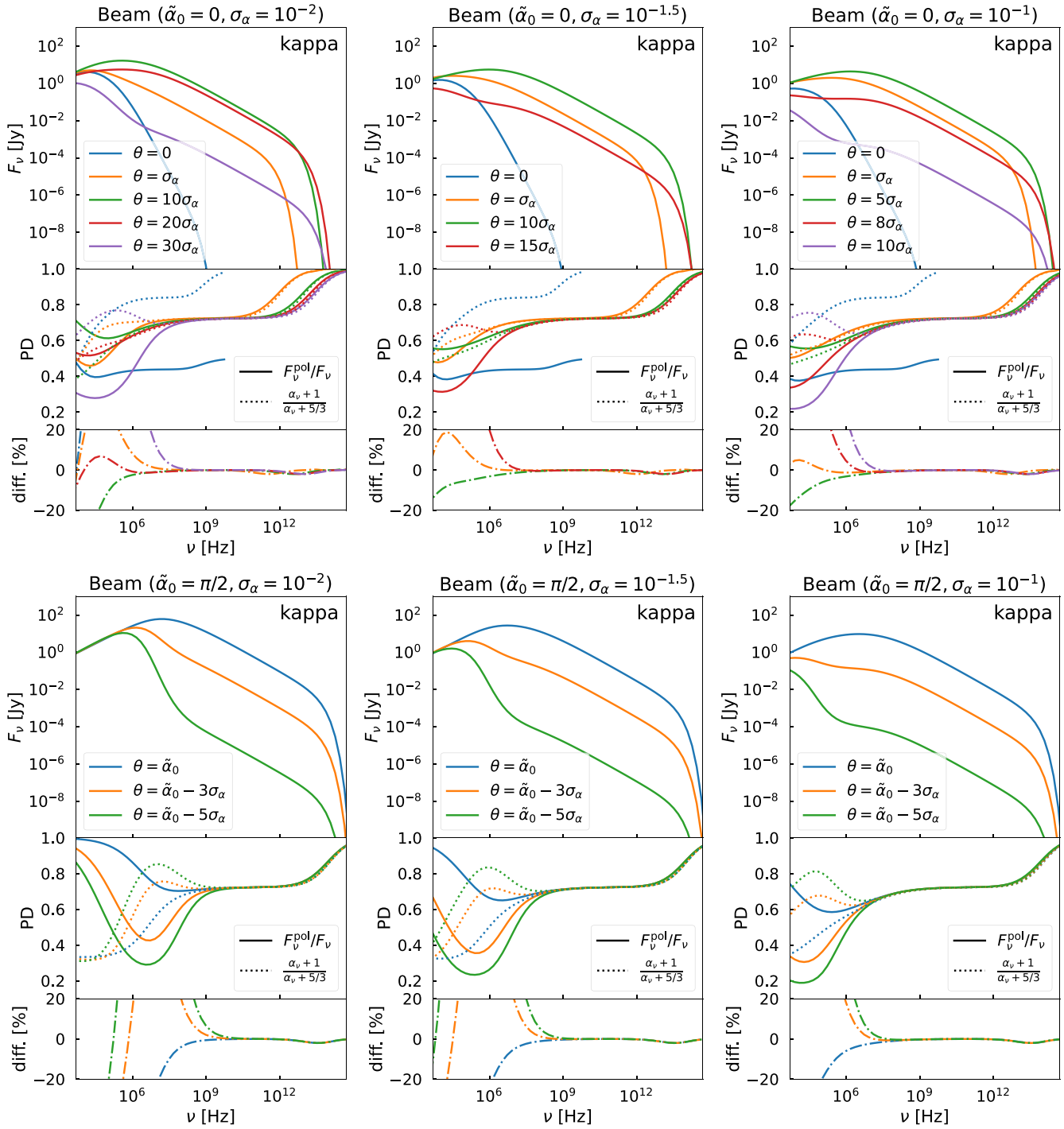

Figure 5. Synchrotron spectra of the beam model with different values of the parameters, i.e. the beaming direction $\tilde{\alpha}_0$, the opening angle of the beam σ_α, and the viewing angle θ. For all the calculations, electrons are assumed to follow a kappa distribution with $\kappa = 3.5$ and $w = 10$, and a high-energy cut-off $\gamma = 10^5$. PD is calculated using two methods. The solid line is calculated using the full formula (equations 6 and 7), and the dotted line is calculated from the local spectral index α_ν (equation 22). The beamwidth of these models are $\alpha_{\rm HWHM} = 0.15, 0.27, 0.49, 0.012, 0.037, 0.12$ from left to right, from top to bottom. Besides, the following parameters are used: $N_{e,0} = 10^{58}$, $B = 1$ mG, and $D = 1$ Gpc.

the particle distribution deviates from isotropy, in the momentum space.

Polarized radiation can be modified in propagation, through Faraday rotation and conversion (see Pacholczyk & Swihart 1967; Sazonov & Tsytovich 1968) and also polarization dependent absorption (see Pacholczyk & Swihart 1967; Jones & O'Dell 1977). Faraday leads to the conversion between two Stokes parameters, U and Q, along a single ray, which alters the polarization angle but does not affect the PD. For an extended synchrotron source with inhomogeneous magnetic-field structure, the total emission is

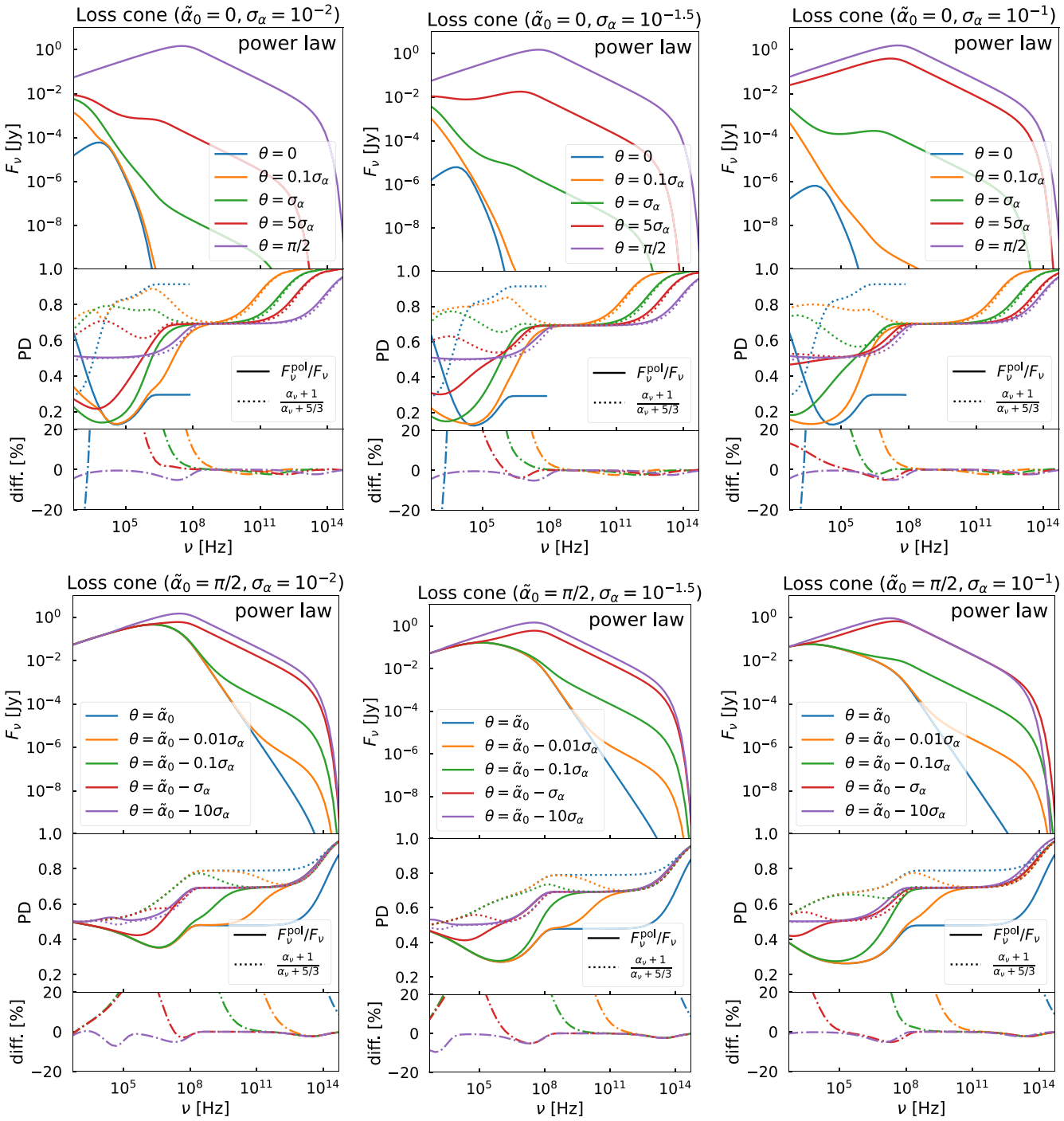

Figure 6. Synchrotron spectra of the loss-cone model with different values of the parameters, i.e. the loss-cone direction $\tilde{\alpha}_0$, the opening angle of the loss cone σ_α, and the viewing angle θ. For all the calculations, electrons are assumed to follow a power-law energy distribution with index $p = 2$, a low-energy cut-off $\gamma = 10^2$, and high-energy cut-off $\gamma = 10^5$. PD is calculated using two methods. The solid line is calculated using the full formula (equations 6 and 7), and the dotted line is calculated from the local spectral index α_ν (equation 22). The cone width of these models are $\alpha_{\rm HWHM} = 0.15, 0.27, 0.49, 0.012, 0.037, 0.12$ from left to right, from top to bottom. Besides, the following parameters are used: $N_{e,0} = 10^{58}$, $B = 1$ mG, and $D = 1$ Gpc.

the sum of contributions of all rays reaching that observer. These rays have different amount of Faraday rotation in their propagation (e.g. when they pass through a turbulent medium) in addition to different initial Stokes U and Q. The measured PD of the emission contributed by a bunch of spatial unresolved rays is therefore always lower than the intrinsic PD of the same set of rays if both the emission region and the medium between it and observer have uniform magnetic field and particle density. This effect would contribute to the so-called beam depolarization in external Faraday dispersion.

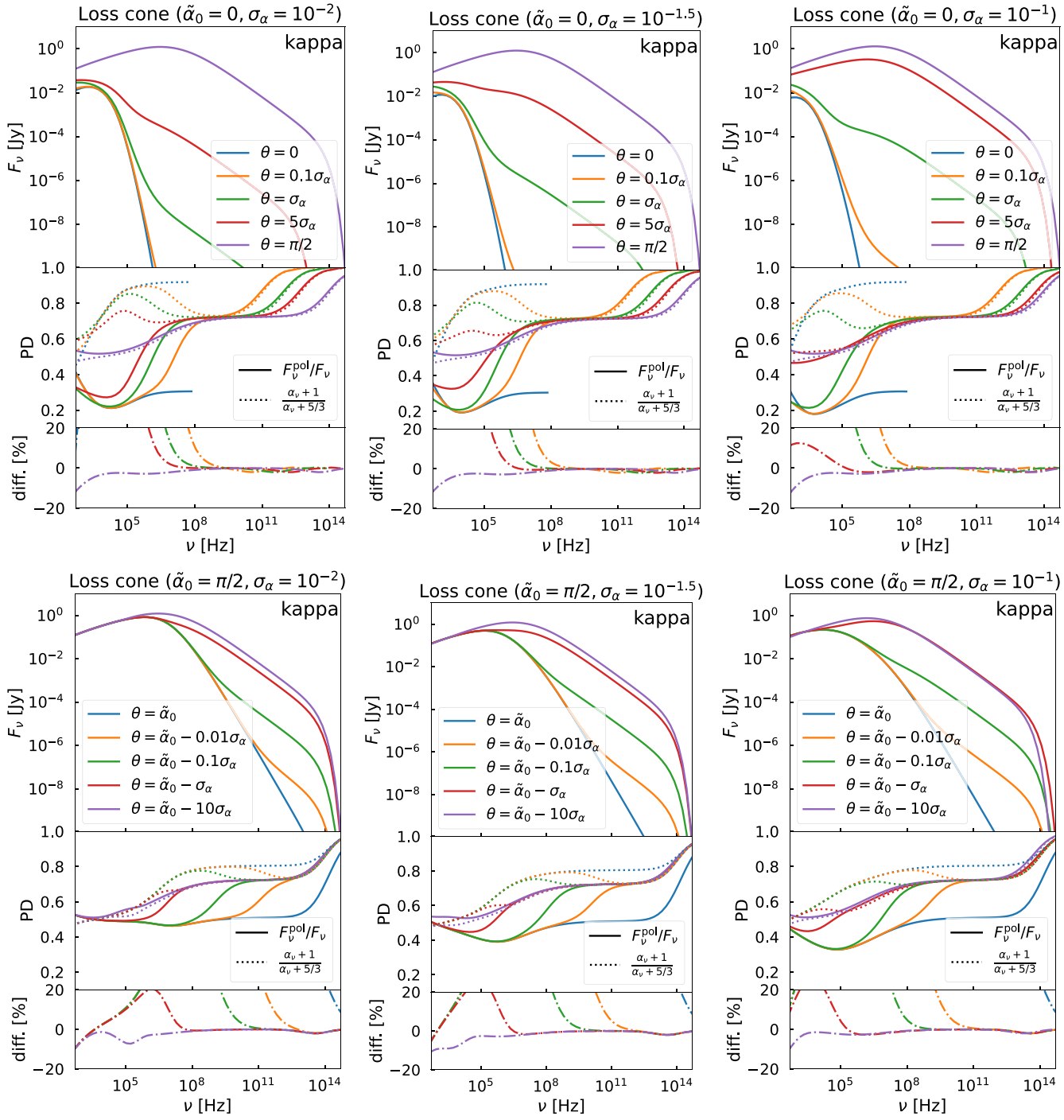

Figure 7. Synchrotron spectra of the loss-cone model with different values of the parameters, i.e. the loss-cone direction $\tilde{\alpha}_0$, the opening angle of the loss cone σ_α, and the viewing angle θ. For all the calculations, electrons are assumed to follow a kappa distribution with $\kappa = 3.5$ and $w = 10$, and a high-energy cut-off $\gamma = 10^5$. PD is calculated using two methods. The solid line is calculated using the full formula (equations 6 and 7), and the dotted line is calculated from the local spectral index α_ν (equation 22). The cone width of these models are $\alpha_{\rm HWHM} = 0.15, 0.27, 0.49, 0.012, 0.037, 0.12$ from left to right, from top to bottom. Besides, the following parameters are used: $N_{e,0} = 10^{58}$, $B = 1$ mG, and $D = 1$ Gpc.

PD, only accounting for linear polarization, can be modified in the presence of inter-conversion between linear polarization and circular polarization modes (see e.g. Pacholczyk 1977; Melrose & McPhedran 1991) and mode-dependent absorption (see Pacholczyk & Swihart 1967; Jones & O'Dell 1977) in propagation. It could also be modified by boundary effects arisen (see e.g. Hecht 2001) for polarized radiation traversing a composite medium, consisting of components with substantial gradients in their refractive indices. This

effect is well known in laboratory physics but is seldom explored in astrophysical settings.[5]

4.2 Practical applications in observations

Equation (1), together with the formula for rotation measure,[6] which is defined as $\mathcal{R} \equiv (\Delta\varphi)\lambda^{-2}$ [where λ is the wavelength of the radiation, and $\varphi = (1/2)\tan^{-1}(U/Q)$] has been a work-horse in astrophysics for the studies of emission of synchrotron sources and the line-of-sight modification of the polarized synchrotron radiation. An 'algorithm' as follows is often used for the interpretations of polarized radiation, in particular in the radio wavelengths as the emission mechanism of many non-thermal source is of synchrotron origin: (1) measure the total fluxes, polarized fluxes, and polarization angle of the radiation from sources at several wavebands. (ii) Make plots of fluxes, polarized fluxes, and polarization angle as function of wavelength for sources. (iii) Deduce p, PD, and $\mathcal{R}$ from the plots. (iv) Apply these information to set constraints on the physical and dynamical processes in the source and on the properties of magnetized medium between the sources and the observers. This algorithm is often based on an implicit assumption that the momentum distribution of the emitting particles is isotropic and they gyrate in a magnetic field in radii much smaller than the length-scale over which the magnetic field varies in the emission region and in the medium the radiation traverses.

Modification of PD can be interpreted as the presence of structural inhomogeneities in the magnetic fields (e.g. global spatial non-uniformity or tangled field lines) or abnormal number density distribution of charged particles (e.g. large density gradients, jumps or turbulence), which are presumably electrons and/or positrons. An extended power law with a positive spectral index α at high frequencies is attributed to optically thin emission. The power-law index α is an indicator of whether or not the charged particles is freshly accelerated (with $\alpha \approx 0.7$) or has aged (with $\alpha \sim 1$ or higher). A spectral turn-over at low frequencies signals an optically thin to optically thick transition, and the frequency at which the radiation peaks is determined by the strength of the magnetic field in the emission region (self-absorption) or in the medium between the source and the observer (external absorption).

Shock acceleration processes generally leads to $p \approx 2.3 - 2.5$ (see Bell 1978; Blandford & Ostriker 1978; Kirk et al. 2000), which corresponds to an intrinsic PD of ∼70 per cent (using equation 1). A 70 per cent PD is commonly considered as the canonical upper limit for synchrotron-emitting astrophysical objects, as the observed values are expected to be lower than that due to structural inhomogeneity and propagation effects as described in Section 4.1. For point sources, the PD of individuals could be contaminated by background and foreground emission from line-of-sight diffuse media, when they are magnetized and their emission is non-negligible compared to sources (see On et al. submitted).

In the standard algorithm α is determined by fitting an extended flux spectrum crossing over a substantial range of wavelengths (or frequencies). It is then used to obtain p and PD. Although it may sound trivial, the reality is that it is not always possible to obtain a sufficient coverage in wavelength (or frequency) in observations to confidently determine α, even when the emission spectrum is actually an extended power law. Moreover, there is no guarantee that the emission spectrum is a power law. Thus, using the value of α obtained from the fit to calculate p and the corresponding PD becomes a meaningless exercise, if the emitting charged particles do not have a power-law energy distribution. Adopting the PD derived from this fit will give misleading interpretation at best and may even lead to incorrect scenarios or physical models.

The findings of our study imply that we can construct more robust algorithms that are reliable beyond an extended power-law spectrum and are applicable when the observations lack broad multiwavelength (multifrequency) coverage. What we need is to determine the local spectral index α_ν, instead of the global spectral index α. The index α_ν is a local quantity, which is well defined at the frequency ν if the spectral segment over ν is sufficiently smooth, unlike α, which is ill defined when the spectrum is not a power law. As shown in Section 3, equation (22), which makes use of α_ν, gives PD that matches the analytical value surprisingly well. Equation (22) is therefore the more general and appropriate expression for intrinsic PD, provided that the momentum distribution of the emitting charged particles is sufficiently isotropic.

4.3 Remarks on momentum isotropy of charged particles

We have demonstrated the versatility of the generalized formula equation (22) for the analysis of polarized synchrotron radiation and inference of the energy distribution of the emitting charged particle, when the radiation does not have an extended power-law spectral segments. The applicability of equation (22) requires that the momentum distribution of emitting charged particles is isotropic. As shown in our calculations the spectral properties of the emission from particles with anisotropic momentum distribution can substantially differ to those of the emission from particles with isotropic momentum distribution. Recent studies highlighted the difference in the spectral properties of the synchrotron radiation for electrons with isotropic and anisotropic momentum (Yang & Zhang 2018; Comisso et al. 2020) [see also an earlier study by Robinson (1985) for a more general plasma and space physics context]. We extend their work to include polarization. Unsurprisingly, the polarization properties of synchrotron radiation from charged particles with isotropic and anisotropic particles can differ substantially, which can be seen in the cases shown in Section 3.2.

[5]For instance, when low-frequency synchrotron radiation traverses a foreground current sheet, such as those associated with a collisionless astrophysical shocks, the PD of the synchrotron radiation will inevitably be affected. Observations have shown that AGNs could have substantial radio synchrotron radiation as low as 100 MHz (see e.g. Calistro Rivera et al. 2017). The study of Singh et al. (2013) on Seyfert galaxies shows that a good fraction of these sources have similar values of spectral indices measured between 240 MHz, 610 MHz, 1.4 GHz, and 5 GHz, hinting that the radio emission from AGN could extend to 100 MHz, provided the radiation is not fully suppressed by the plasma-frequency cut-off of the line-of-sight medium.

[6]In a magnetized plasma with a spatially varying magnetic field $\boldsymbol{B}$, an expression for the rotation measure accounting for both thermal and non-thermal electrons is given by

$$\mathcal{R}(s) = \frac{e^3}{2\pi {m_\mathrm{e}}^2 c^4} \int_{s_0}^{s} \mathrm{d}s'\, n_\mathrm{e}(s')\Theta(s')B_\parallel(s') \tag{24}$$

(see On et al. 2019), where the electrons have an isotropic momentum distribution and a total number density n_e. The variable $\Theta(s) = 1 - \Upsilon(s)[1 - \zeta(p, \gamma_\mathrm{i})]$ is a factor weighing the contribution of thermal and non-thermal electrons, given the fraction of non-thermal electron $\Upsilon(s) = n_{\mathrm{e,nt}}(s)/n_\mathrm{e}(s)$. For non-thermal electrons with a power-law energy distribution of an index p,

$$\zeta(p, \gamma_\mathrm{i}) = \frac{(p-1)(p+2)}{(p+1)} \left(\frac{\ln \gamma_\mathrm{i}}{{\gamma_\mathrm{i}}^2}\right) \tag{25}$$

(for $p > 1$), where γ_i is the Lorentz factor of low-energy cut-off of the non-thermal electrons.

In modelling of radiation from astrophysical sources, the momentum distribution of the emitting particles is often assumed to be isotropic, for simplicity or for avoiding unmanageable complications especially when we lack information about the exact microscopic properties regarding the emission charged particle distribution. In certain situations, the assumption of isotropic momentum distribution is reasonable, e.g. when the charged particles are scattered stochastically by turbulent magnetic fields. In many astrophysical situations, the momentum distribution of the charged particles would have some degree of anisotropy. As pointed out in Yang & Zhang (2018), momentum distribution anisotropy can arise from anisotropic accelerations such as in relativistic shock waves with a spatially ordered magnetic field. Phenomena such as magnetic reconnection and magnetic mirroring can also cause anisotropy in the particle momentum distribution (see Yang & Zhang 2018; Comisso & Sironi 2019; Lazarian & Xu 2021; Xu & Lazarian 2023). Momentum anisotropy can also arise from strong radiative cooling (Comisso & Sironi 2021) and from propagation of relativistic charged particles in certain electromagnetic field configurations (cf. the developing of loss-cone and horseshoe momentum distribution as those in the cyclotron maser sources, see Melrose & Dulk 1982; Ergun et al. 2000; Willes & Wu 2004, for example). In addition, anisotropic electrons provide explanations to some of the astrophysical phenomenon, such as the limb-brightening of AGN jets (Tsunetoe et al. 2025).

Comisso & Jiang (2023) presented polarization calculations of synchrotron radiation from charged particles with anistropic momentum distribution with a power-law energy spectrum. A more general and comprehensive exploration of the effects on polarization properties of synchrotron radiation from charged anisotropic momentum distribution for various energy spectra is presented in this work. Similar to Comisso & Jiang (2023), we have found that the polarization properties are strongly affected by the anisotropic particle momentum, and therefore the canonical upper limit of roughly 70 per cent for optically thin synchrotron radiation would deem to be inapplicable in many astrophysical situations where isotropic momentum of the charged particles are not guaranteed (see Yang & Zhang 2018; Comisso & Jiang 2023). It is important to be cautious on the conditions for the applicability of certain equations in relating the PD and spectral properties in synchrotron sources in astrophysics and in imposing the canonical limits of PD derived from the assumption of isotropic momentum distribution and an extended power-law energy spectrum of the emitting charged particles.

4.4 Synchrotron radiation emitted by other charged particles

We have presented the calculations for the spectropolarization of synchrotron radiation from electrons with various energy distributions, relaxing the restriction that the electrons have an isotropic momentum distribution. In astrophysical systems, relativistic electrons are not the only emitters of polarized synchrotron radiation. Pairs are common in relativistic astrophysical plasmas as the energetic particles would exceed the 1-MeV threshold. The results that we have obtained from synchrotron radiation for electrons are directly applicable to synchrotron radiation for positrons, as all the expressions have no dependence on the odd power of particle charges. In violent astrophysical sources, e.g. gamma-ray bursts and relativistic jets/outflows in some AGNs, heavier charged particles, such as muons and protons, could be present, and these particles are also emitter of synchrotron radiation. When there are substantial amounts of these particles, their radiation would have noticeable contribution to the spectral energy distributions of the sources (see e.g. Cerruti et al. 2015; Sahakyan et al. 2023; Xue et al. 2023; Zhang et al. 2025).

We note that with appropriate scaling, the results obtained for electrons and positrons can be generalized for the other charged particles. In the classical theory of radiation, the essential parameters in the emitting particles, denoted as X are their mass $m_{\rm X}$ and their electric charge $q_{\rm X}$. For synchrotron process, the frequency of the radiation scales with the charge-to-mass ratio $(q_{\rm X}/m_{\rm X})$, of the particles, when their Lorentz factor is fixed. The power of radiation scales with the Thomson cross-section, which is proportional to $(q_{\rm X}{}^2/m_{\rm X})^2$, of the particles, and hence the scaling factor is $(q_{\rm X}{}^2/m_{\rm X})^2$. In a heuristic argument, for charged particles, with either isotropic or anisotropic momentum pitch-angle distributions, the expressions that we have obtained in Section 2.1 could be expressed in a generalized form, in term of $q_{\rm X}$ and $m_{\rm X}$, with electrons as the special case, where $q_{\rm X} = e$ and $m_{\rm X} = m_{\rm e}$. The generalized expressions for arbitrary charged particles X are the same expressions as those shown in Section 2.1 but with e replaced by $q_{\rm X}$ and m_e by $m_{\rm X}$.

The generalized formula $\Pi_{\rm L,gen} = (\alpha_\nu + 1)/(\alpha_\nu + 5/3)$ (equation 22) is also applicable to all charged particles with an isotropic pitch-angle distribution. For anisotropic distributions, it is still applicable to the high-frequency range for some cases, but one must be careful how this frequency range shifts according to the charge and mass of the emitting particles. The most important implication is that, if the observed radiation is evidently synchrotron radiation, the generalized PD formula can be applied regardless of the identity of the emitting particles, given the assumption that the pitch-angle distribution is isotropic.

5 CONCLUSIONS

We have generalized the commonly employed formula $\Pi_{\rm L,pl} = (p + 1)/(p + 7/3) = (\alpha + 1)/(\alpha + 5/3)$ for determining the degree of linear polarization of synchrotron sources in this work. We show that when the global spectral index α is replaced by α_ν, which is locally defined, the generalized PD formula $\Pi_{\rm L,gen} = (\alpha_\nu + 1)/(\alpha_\nu + 5/3)$ will give an excellent approximation to the degree of linear polarization obtained by direct emissivity calculations, provided that the emitting charged particles have an isotropic momentum distribution. The new formula that we present provides a reliable tool in the prediction and in the interpretation of the polarization properties of astrophysical synchrotron sources when observations do not have a broad-band coverage in frequencies or in wavelengths. We also conduct calculations of linear polarization of synchrotron radiation from charged particle with anisotropic momentum distribution. We present results of two special cases: the beamed distribution and the loss-cone distribution. Our calculations have shown that both the total and the polarized intensity differ to those of correspondence cases where the charged particles have isotropic momentum. We note that for anisotropic distributions, the generalized formula that we present may works for a certain frequency range, and is generally inapplicable at the low frequencies. This indicates that the anisotropy in the momentum distribution of the emitting particles would need to be taken in consideration when interpreting the spectral polarimetric data of astrophysical synchrotron radiation sources.

ACKNOWLEDGEMENTS

We thank Dr Po Kin Leung (CUHK) for valuable discussions on radiative processes in astrophysical systems. We thank the referee for the useful suggestion. PCWL was supported by a UCL Graduate Research Scholarship and a UCL Overseas Research Scholarship. KJL was supported by a PhD Scholarship from the Vinson and Cissy Chu Foundation and by a UCL MAPS Dean's Prize. YXJY

and AKHK are supported by National Science and Technology Council of the Republic of China (Taiwan) through the grant 113-2112-M-007-001. KW acknowledges the support from the ANU Distinguished Visitor award and thanks the hospitality of the ANU Research School of Astronomy and Astrophysics and Centre for Gravitational Astrophysics during his visits and thanks the hospitality of the NTHU IoA, where part of this work was conducted, during his visits. PCWL, YXJY, and KW acknowledge the support from the UCL Cosmoparticle Initiative. This research has made use of NASA's Astrophysics Data System.

DATA AVAILABILITY

No new data were generated or analysed in support of this research.

REFERENCES

Baldwin D. E., 1977, Rev. Mod. Phys., 49, 317
Bell A. R., 1978, MNRAS, 182, 147
Blandford R. D., Ostriker J. P., 1978, ApJ, 221, L29
Calistro Rivera G. et al., 2017, MNRAS, 469, 3468
Cerruti M., Zech A., Boisson C., Inoue S., 2015, MNRAS, 448, 910
Chan J. Y. H., Wu K., On A. Y. L., Barnes D. J., McEwen J. D., Kitching T. D., 2019, MNRAS, 484, 1427
Coburn W., Boggs S. E., 2003, Nature, 423, 415
Comisso L., 2024, ApJ, 972, 9
Comisso L., Jiang B., 2023, ApJ, 959, 137
Comisso L., Sironi L., 2019, ApJ, 886, 122
Comisso L., Sironi L., 2021, Phys. Rev. Lett., 127, 255102
Comisso L., Sobacchi E., Sironi L., 2020, ApJ, 895, L40
Davelaar J., Mościbrodzka M., Bronzwaer T., Falcke H., 2018, A&A, 612, A34
Dermer C. D., Cerruti M., Lott B., Boisson C., Zech A., 2014, ApJ, 782, 82
Ergun R. E., Carlson C. W., McFadden J. P., Delory G. T., Strangeway R. J., Pritchett P. L., 2000, ApJ, 538, 456
Event Horizon Telescope Collaboration, 2022, ApJ, 930, L16
Fromm C. M. et al., 2022, A&A, 660, A107
Fuerst S. V., Wu K., 2004, A&A, 424, 733
Ginzburg V. L., Syrovatskii S. I., 1965, ARA&A, 3, 297
Ginzburg V. L., Syrovatskii S. I., 1969, ARA&A, 7, 375
Hecht E., 2001, Optics 4th edition, Wesley Publishing Company, MA
Jones T. W., O'Dell S. L., 1977, ApJ, 214, 522
Kaaret P. et al., 2024, ApJ, 961, L12
Kardashev N. S., 1962, Soviet Astron., 6, 317
Kirk J. G., Guthmann A. W., Gallant Y. A., Achterberg A., 2000, ApJ, 542, 235
Krennrich F. et al., 1999, ApJ, 511, 149
Lai P. C. W., Ng C. Y., Bucciantini N., 2022, ApJ, 930, 1
Landau R. et al., 1986, ApJ, 308, 78
Lazarian A., Xu S., 2021, ApJ, 923, 53
Massaro E., Perri M., Giommi P., Nesci R., 2004, A&A, 413, 489
Melrose D. B., Dulk G. A., 1982, ApJ, 259, 844
Melrose D. B., McPhedran R. C., 1991, Electromagnetic Processes in Dispersive Media. Cambridge University Press, Cambridge, UK
On A. Y. L., Chan J. Y. H., Wu K., Saxton C. J., van Driel-Gesztelyi L., 2019, MNRAS, 490, 1697
Pacholczyk A. G., 1977, in International Series on Natural Philosophy. Vol. 89, Pergamon Press, Oxford
Pacholczyk A. G., Swihart T. L., 1967, ApJ, 150, 647
Pandya A., Zhang Z., Chandra M., Gammie C. F., 2016, ApJ, 822, 34
Perlman E. S. et al., 2011, ApJ, 743, 119
Prather B. S. et al., 2023, ApJ, 950, 35
Robinson P. A., 1985, Plasma Phys. Control. Fusion, 27, 1037
Rybicki G. B., Lightman A. P., 1979, Radiative Processes in Astrophysics. Wiley, New York
Sahakyan N., Giommi P., Padovani P., Petropoulou M., Bégué D., Boccardi B., Gasparyan S., 2023, MNRAS, 519, 1396
Saxton C. J., Wu K., Korunoska S., Lee K.-G., Lee K.-Y., Beddows N., 2010, MNRAS, 405, 1816
Sazonov V. N., Tsytovich V. N., 1968, Radiophys. Quantum Electron., 11, 731
Singh V., Shastri P., Ishwara-Chandra C. H., Athreya R., 2013, A&A, 554, A85
Slane P., Ferrazzoli R., Zhou P., Vink J., 2024, Galaxies, 12, 59
Soffitta P. et al., 2021, AJ, 162, 208
Tramacere A., Massaro F., Cavaliere A., 2007, A&A, 466, 521
Tsunetoe Y., Pesce D. W., Narayan R., Chael A., Gelles Z., Gammie C., Quataert E., Palumbo D., 2025, ApJ, 984, 35
Tucker W., 1975, Radiation Processes in Astrophysics. MIT Press, Cambridge
Weisskopf M. C. et al., 2022, J. Astron. Telesc. Instrum. Syst., 8, 026002
Westfold K. C., 1959, ApJ, 130, 241
Willes A. J., Wu K., 2004, MNRAS, 348, 285
Xu S., Lazarian A., 2023, ApJ, 942, 21
Xue R., Huang S.-T., Xiao H.-B., Wang Z.-R., 2023, Phys. Rev. D, 107, 103019
Yang Y.-P., Zhang B., 2018, ApJ, 864, L16
Younsi Z., Wu K., Fuerst S. V., 2012, A&A, 545, A13
Zhang B. T., Murase K., Ioka K., Zhang B., 2025, J. High Energy Astrophys., 45, 392

APPENDIX A: ISOTROPIC MONO-ENERGY ELECTRONS

For isotropic mono-energy particle distribution, the total intensity is proportional to $F(x)$ and the polarized intensity is proportional to $G(x)$, where $x = \nu/\nu_c$. The PD is therefore $= G(x)/F(x)$. Fig. A1 shows the total and polarized synchrotron spectrum, and the PD calculated using two methods. It shows that the generalized formula PD $= (\alpha_\nu + 1)/(\alpha_\nu + 5/3)$ works well even for the mono-energy case. This is surprising given that the formula is originally derived from an infinitely extended power law. It is unclear what the physical or mathematical reasons are behind the validity of this formula.

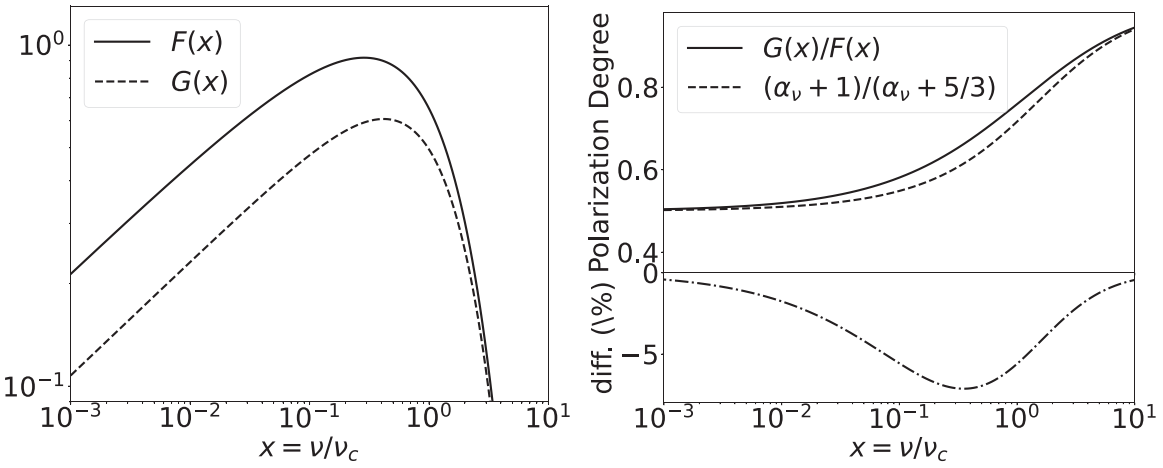

Figure A1. Synchrotron emission of isotropic mono-energy electrons. *Left*: Total flux (solid line) and polarized flux (dashed line) of the synchrotron emission with arbitrary normalization in flux. *Right*: Polarization degree calculated analytically versus using the generalized PD formula. The percentage difference of these two methods is always smaller than 7 per cent.

APPENDIX B: CALCULATING THE POLARIZED EMISSION USING MODELS IN YANG & ZHANG (2018)

In Yang & Zhang (2018), they studied how anisotropic distribution of electrons changes the total power of the synchrotron spectrum. One purpose of this work is to also examine the impact on the polarized emission for electrons with anisotropic distribution. We think it would be good idea to replicate their models with polarization calculations included.

There are a couple of differences between their work and our work. One is that they have an additional $1/\sin^2\tilde{\alpha}$ factor in equations (2) and (3) to account for the difference in received and emitted power (Rybicki & Lightman 1979). As we discussed in the main text, whether to include this factor depends on the astrophysical context. The inclusion of $1/\sin^2\tilde{\alpha}$ implicitly indicates that they considered a uniform magnetic field with electrons moving in perfect helical motion within the magnetic field. In addition, they considered electrons with a bulk motion, parametrized by the Doppler factor δ_D. We herein reproduce their model shown in fig. 5 in Yang & Zhang (2018), in which electrons follow a power-law distribution with anisotropic distribution modelled as

$$g_e(\tilde{\alpha}) = \frac{1}{\sqrt{2\pi\sigma^2}} \exp\left(-\frac{(\sin\tilde{\alpha} - \sin\tilde{\alpha}_0)^2}{2\sigma^2}\right) . \quad \text{(B1)}$$

The particle energy distribution follows a power law with index $p = 2$, lower cut-off $\gamma_1 = 10^2$, and higher cut-off $\gamma_2 = 10^3$. Fig. B1 is calculated following the recipe in Yang & Zhang (2018). Fig. B1 shows the total power and the PD of the synchrotron radiation using their model. The left panel is the same as fig. 5 in Yang & Zhang (2018). The results show that, even if the electrons follow a power-law distribution, the anisotropy in momentum distribution causes very different total power spectrum and polarization property.

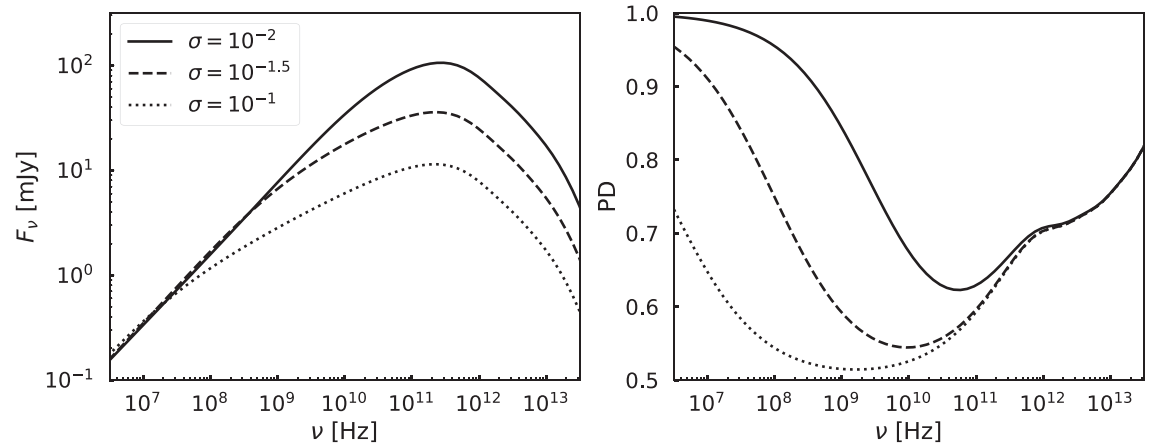

Figure B1. Reproducing fig. 5 in Yang & Zhang (2018) and extending the calculation to polarization. The model parameters are: the power-law lower cut-off $\gamma_1 = 10^2$, the power-law upper cut-off $\gamma_2 = 10^3$, the power-law index $p = 2$, the pitch-angle distribution model parameters $\sigma = 10^{-1}, 10^{-1.5}, 10^{-2}$ and $\tilde{\alpha}_0 = \pi/4$, the viewing angle $\theta = \pi/4$, $B = 1$ G, $\delta_D = 10$, $N_{e,0} = 10^{48}$, and $D = 1$ Gpc.

This paper has been typeset from a TEX/LATEX file prepared by the author.